行政院國家科學委員會補助專題研究計畫 □成果報告 ☑期中進度報告

（計畫名稱）

Study of terahertz generation processes in doped GaSe crystals

計畫類別：☑ 個別型計畫　□ 整合型計畫
計畫編號：NSC 96－2923－M－009－001－MY3
執行期間：96 年 8 月 01 日至 99 年 7 月 31 日

計畫主持人：羅志偉
共同主持人：吳光雄、莊振益
計畫參與人員：古新安

成果報告類型(依經費核定清單規定繳交)：☑精簡報告　□完整報告

本成果報告包括以下應繳交之附件：
□赴國外出差或研習心得報告一份
□赴大陸地區出差或研習心得報告一份
□出席國際學術會議心得報告及發表之論文各一份
□國際合作研究計畫國外研究報告書一份

處理方式：除產學合作研究計畫、提升產業技術及人才培育研究計畫、列管計畫及下列情形者外，得立即公開查詢
□涉及專利或其他智慧財產權，□一年□二年後可公開查詢

執行單位：交通大學 電子物理系

中　華　民　國　97 年　5 月　28 日

1. Contents:

1-1. **Background**

Recently, there is growing interesting in fields using terahertz (THz) waves, or T-rays, for spectroscopy, imaging, communications, signal processing, and quantum information. The prospects of T-rays applications could be imaged by the lifelike cover picture (Fig. 1) of Rensselear Magazine [1]. Why do they call it "Next Rays"? In the viewpoint of safety, the T-rays will not cause harmful photoionization in biological tissues due to their low photon energies (4 meV@ 1THz, one millions times weaker than an x-ray photon). Moreover, numerous organic molecules have rotational and vibrational transitions which lead to strong absorption and dispersion in the region from GHz to THz. These characteristics are specific to the targets and enable T-rays fingerprinting. So T-rays are the wave of the future. In the pass decade, this previously hidden region of the electromagnetic spectrum has caught the imagination of scientists around the world.

T-rays are not only used to investigate scientific researches such as physics, chemistry, plasma fusion diagnostics, electron bunch diagnostics, THz wave microscope, etc., but also applied to commercial fields--- skin imaging for cancer detection, mail inspection, luggage inspection, non-contact and non-destructive method for example. After 911 in USA, everyone attaches great importance to the security everywhere. Of course, T-rays have been the most perspective candidate for defense, e.g. homeland security, explosives detection, see-through wall, imaging in space using satellites, chemical and biological agents detection.

Terahertz domain of electromagnetic radiation spectrum (approximately 15 μm – 10 mm or 0.03 – 20 THz) is located between mid IR and microwave range and remains comparatively low investigated. That is connected with technical and technological difficulties in creation of corresponded element base (radiating and detecting devices, lenses, filters etc.). On the other hand terahertz radiation possesses a set of important for practical applications properties. For instance it has higher penetrating power then optical radiation and allows more detailed imaging than microwaves. It can propagate through most of non-metallic and non-polar media. Many characteristic features of different substances lie in this range, for instance rotational and oscillating frequencies of molecules. On the base of THz radiation source it is possible to create a remote detector of explosive substances with high spatial resolution. Terahertz spectroscopy becomes an important tool of molecular biology, electrophysics, medicine etc.

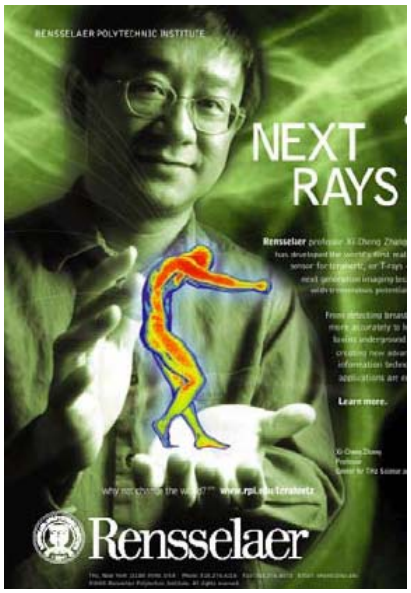

Fig. 1 the applications of THz are shown in the cover picture of Rensselear Magazine.

Early research concentrated on the generation and detection of THz radiation. By present time one can get terahertz radiation by dipole antennas [2-4], from semiconductor surface [5], by gas lasers with optical pump [6], free-electron lasers [7], and quantum-cascade lasers [8]. All methods have their merits and deficiencies. It is possible to obtain broad-band radiation with microwave lamps, but it is not coherent, free-electron lasers allows to get radiation in wide range and with high output power, but they are not compact and expensive thus being not available for most of research laboratories.

A way to create relatively compact and not expensive coherent terahertz radiation source is nonlinear optical conversion in nonlinear crystals. By the moment the best results, in terms of tuning range and peak output powers are obtained on GaSe and $ZnGeP_2$ crystals

[9, 10]. Tuning range of some thousands of micrometers and peak powers of some hundreds of watts were achieved. On the other hand the task of optimizing the crystal properties is real. GaSe possesses low mechanical properties, as it is layered and easy cleavable material, which makes a task to grow long homogeneous crystal difficult and do not allow to produce optical surfaces at angles to optical axis, that is needed for optimization of some types of frequency converters. Also $ZnGeP_2$ has rather low transparency and refractive indices.

GaSe crystals have being grown since 1960s. Original technology of manufacturing was developed by lab the participant of the project. The crystals are commercially available and used by many research labs for IR and THz applications. It was shown that doping could improve mechanical and optical properties of the materials.

1-2 Goals

This project is directed towards finding of mechanisms, determining efficiency of terahertz radiation generation in nonlinear optical semiconducting crystals GaSe at employing of two principally possible methods of generation: generation at fast current changing determined by non-equilibrium carriers at excitation by short-pulse laser and generation at nonlinear conversion of IR-laser radiation, as well as finding and explanation of regularities in this efficiency dependencies on crystal compound and growth conditions. From the practical point of view the basic objective of the project is designing of method to obtain the crystals with enhanced set of properties for terahertz radiation generation.

GaSe crystals which will be the main subject of the research within this project are among the most prospective IR-range crystals. In last years the possibility to create tunable terahertz generation sources on its base was shown experimentally. GaSe possesses the lowest absorption in the terahertz range among known nonlinear crystals. Therefore the crystals are prospective for THz generation by nonlinear-optical conversions (difference frequency generation). On the other hand the efficiency of conversion and in turn the power of output radiation is limited by crystal properties such as optical transparency and homogeneity. In particular at DFG the increasing crystal length must give higher conversion efficiency that is not observed in real experiments. The answer should be given what limits the possibilities of the crystals and whether it is possible to improve them, for example by introducing chemical elements with bigger atomic radius and higher polarizability. The second method to generate THz is employing of dipole antenna scheme. For enhancement of efficiency of such devices it is necessary to use materials with high resistance and carrier mobility. Electrical transport properties of GaSe can be considerably modified by doping and it looks reasonable to investigate dipole antennas based on doped crystals, which also should give information on their electronic properties.

Within the project it is planed to find conditions of growth of large homogeneous GaSe crystals with lower absorption in THz region and investigation of possibilities to enhance their characteristics by the way of their doping for creation on their base of optical elements for THz range generators and frequency converters. In particular the problem is to reveal the mechanisms determining the optical transparency of nonlinear optical crystals in the specified range. After getting the suitable nonlinear optical crystals for high power and widely tunable wavelength THz generation, we could study the ultrafast dynamics in some interesting materials such as high Tc superconductor, multiferroics manganites, magnetic semiconductors and semiconductor quantum dots etc..

Finally the task is to develop scientifically based and stable schemes to produce nonlinear optical single crystals with improved parameters for applications in the THz range.

1-3 Results

(1) In Russia:

The S-doped GaSe crystals have been grown by the way of modified two-temperature method (horizontal variant). An initial component: Gad, Se, and S of high purity (99.9999 %) are used for synthesis in evacuated up to 10^{-5} mm Hg quartz ampoules, the geometry of which is represented in Fig. 2. Weight of charges is about 100-150 grams. Gallium charge is located in separate boat, volume of which allowed containing the whole melt of synthesized GaSe. Doping of crystals by isovalent dopant of sulfur is reached by the way of introduction of a various amount of the dopant in boat with gallium at synthesis of the compound. Process of synthesis includes three sequential stages; its temperature conditions are also represented in Fig. 2. At conditions of the Regime 1 an effective sublimation of selenium atoms in a vapor phase and their interaction with a melt of gallium are realized or, in other words, a synthesis of compound GaSe at safe pressure of selenium vapour in a reactionary ampoule is ensured. The conditions of the Regime 2 ensure homogenization of a melt. And in conditions of the Regime 3 a cooling of a melt is put into effect and a growth of homogeneous ingots of doped GaSe is ensured.

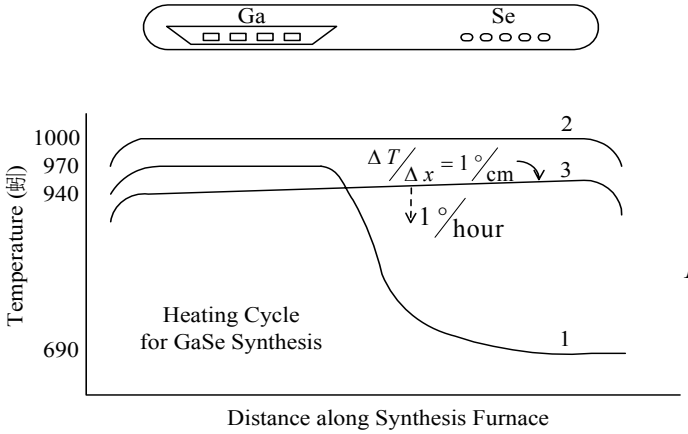

Fig. 2 Cross section view of reactionary ampoule and temperature conditions of Gallium Selenide synthesis.

Growth of the single crystals from melts of synthesized materials by vertical variant of the Bridgman method. Time-temperature regimes of the crystal growth process are identified from phase diagrams of the Ga-Se systems. In accordance with these diagrams and singularities of homogeneity region, the melting of Gallium Selenide has a congruent character, and the compound is low-volatile and narrow-homogeneous phase. Experimental set-up and chosen temperature distribution profile in the GaSe growth furnace are represented in Fig. 3. Evacuated quartz ampoules with an interior diameter of 15-25 mm are used. It was defined that obtaining of GaSe single crystals is ensured at use of following temperature-temporary conditions:

- Growth rate is within 0.5-1 mm/hour.
- Melt temperature is within 1010-1020 ^{o}C;
- Temperature gradient at the crystallization front is 10 degree/cm;

Specimens with thickness of 0.5 mm and 1.0 mm were made for investigation of physical properties and study of frequency conversion processes by exfoliation method from grown single crystal boulles. A few millimetres to few centimetres sized specimens of mixed crystals were made by mechanical methods: diamond saw cut and mechanical polishing, so as it fixing on a metal substrate with the aperture of 5-10 mm in diameter for preservation of specimen flatness. The specifications of all specimens were listed in

Table 1.

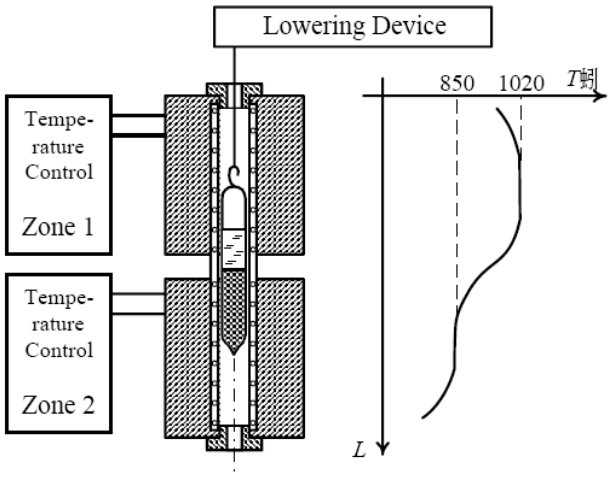

Fig. 3 Experimental set-up is on the left hand and temperature distribution profile in the growth furnace on the right hand of the figure.

Table 1

№	Material	Type	Nominal sulfur concentration, mass. %	Length, mm
1	$GaSe_{0.98}S_{0.02}$	Optical element in holder, aperture dia 7 mm	0.5	1
2	$GaSe_{0.95}S_{0.05}$	Optical element in holder, aperture dia 7 mm	1	1
3	$GaSe_{0.87}S_{0.13}$	Optical element in holder, aperture dia 7 mm	3	1
4	$GaSe_{0.78}S_{0.22}$	Optical element in holder, aperture dia 7 mm	5	1
5	$GaSe_{0.7}S_{0.3}$	Optical element in holder, aperture dia 7 mm	7	1
6	$GaSe_{0.6}S_{0.4}$	Optical element in holder, aperture dia 7 mm	10	1
7	$GaSe_{0.98}S_{0.02}$	Wafer, 1 cm^2	0.5	1
8	$GaSe_{0.98}S_{0.02}$	Wafer, 1 cm^2	0.5	0.5
9	$GaSe_{0.98}S_{0.02}$	Wafer, 1 cm^2	0.5	0.5
10	$GaSe_{0.95}S_{0.05}$	Wafer, 1 cm^2	1	1
11	$GaSe_{0.95}S_{0.05}$	Wafer, 1 cm^2	1	0.5
12	$GaSe_{0.95}S_{0.05}$	Wafer, 1 cm^2	1	0.5
13	$GaSe_{0.87}S_{0.13}$	Wafer, 1 cm^2	3	1
14	$GaSe_{0.87}S_{0.13}$	Wafer, 1 cm^2	3	0.5
15	$GaSe_{0.87}S_{0.13}$	Wafer, 1 cm^2	3	0.5
16	$GaSe_{0.78}S_{0.22}$	Wafer, 1 cm^2	5	1
17	$GaSe_{0.78}S_{0.22}$	Wafer, 1 cm^2	5	0.5
18	$GaSe_{0.78}S_{0.22}$	Wafer, 1 cm^2	5	0.5
19	$GaSe_{0.7}S_{0.3}$	Wafer, 1 cm^2	7	1
20	$GaSe_{0.7}S_{0.3}$	Wafer, 1 cm^2	7	0.5
21	$GaSe_{0.7}S_{0.3}$	Wafer, 1 cm^2	7	0.5
22	$GaSe_{0.6}S_{0.4}$	Wafer, 1 cm^2	10	1
23	$GaSe_{0.6}S_{0.4}$	Wafer, 1 cm^2	10	0.5
24	$GaSe_{0.6}S_{0.4}$	Wafer, 1 cm^2	10	0.5

(1) In Taiwan:

In order to generate the tunable CW THz radiation, a collinear output and tunable dual-wavelength CW Ti:sapphire laser with a simple cavity configuration has been developed in this project. The wavelength splitting range is easily tuned from 10 nm to 120 nm, which provides 56 THz bandwidth for terahertz generation. The total output power of two colors with the spatial mode of TEM_{00} is between 700 mW and 300 mW, for small and large wavelength splittings, respectively, under 5 W argon-ion laser pumping.

Figure 4 shows the collinear, tunable dual-wavelength, CW Ti:sapphire laser cavity. It consists of a standard X-configuration resonator and was pumped by an argon-ion laser (Coherent Innova 90) with an output power of 5 W. The 5mm-long Brewster-cut Ti:sapphire crystal was doped with Ti^{+3} ions at the relative concentration of 0.1%. The curvature radius of the focusing mirrors (M1 and M2 in Fig. 4), at the both ends of the Ti:sapphire crystal, was 10 cm. Their tilted angles were 9° and 8.5° respectively. The pump beam (Ar^{+} laser) was focused onto the crystal by a lens (L1 in Fig. 4) of 10 cm focal length. The reflectivity of output-coupler (M3 in Fig. 4) was 95%, which was coated at 780 nm with 100 nm spanning.

The prime concept is to expand all wavelengths emitted from a Ti:sapphire crystal in free space by the optical dispersion components. Thus it is possible to select the lasing wavelength inside the cavity through a simple mechanism. In our dual-wavelength CW Ti:sapphire laser, a needle-shaped blocker was used as the wavelength selector shown in the inset of Fig. 4. One pair of prisms (P1 and P2 in Fig. 4) was inserted into the long arm of X-configuration resonator to introduce spatial dispersion. The first prism (P1 in Fig. 4) spreads all lasing wavelengths in free space. Then, the second prism (P2 in Fig. 4) collimates all of these wavelengths to the total-reflectivity end mirror (M4 in Fig. 4).

To begin with, we adjusted the all of the optical components in cavity to optimize the output power in single wavelength operation. Afterward the needle-shaped blocker was moved carefully into the laser beam, in front of the total-reflectivity end mirror, from the underside of the laser beam. It was separated into two beams between the first prism and the end mirror. The difference of two wavelengths can be tuned by varying the distance between the two beams by adjusting the vertical position of needle-shaped blocker. The collinear and dual-wavelength laser was delivered from the other arm including output-coupler in the X-configuration resonator. Its spectrum has been measured directly by a spectrum analyzer (Advantest, model Q8384).

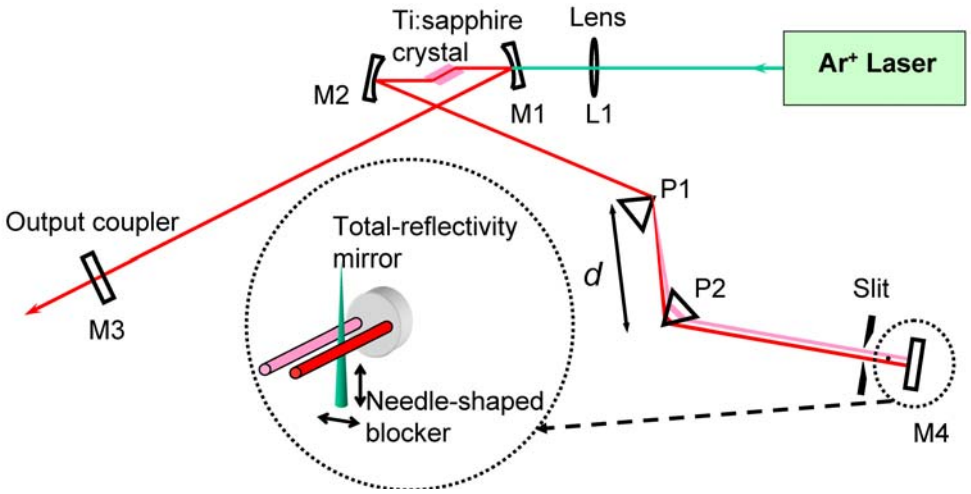

Fig. 4 Schematics of the resonator design of the collinear dual-wavelength CW Ti:sapphire laser. M1 and M2 are the curvature mirrors. M3 is the output coupler with 780 nm coating. M4 is the total-reflectivity end mirror. P1 and P2 are the prisms. L1 is the lens for Ar^{+} laser. d is the distance between P1 and P2.

The inset (a) of Fig. 5 shows that the spatial mode of the tunable dual-wavelength CW Ti:sapphire laser cavity is TEM_{00} which was measured by the beam profiler just after the output coupler (M3 in Fig. 4). Its propagation along the normal direction of output coupler is Gaussian (solid squares in Fig. 5) and its beam quality (M^2) is 1.28. Furthermore, the same output laser beam had been guided into a prism and measured by the beam profiler after that prism. The spatial modes are still TEM_{00} for both wavelengths, λ_1 = 840 nm and λ_2 = 760 nm, as shown in the inset (b) of Fig. 5. They also propagate along the normal direction of output coupler with Gaussian (solid and open circles in Fig. 5). Additionally, the beam qualities (M^2) of λ_1 (840 nm) and λ_2 (760 nm) are 1.20 and 1.18, respectively. This strongly indicates that the output laser beams of both wavelengths are absolutely collinear. For the detail, please refer to the appendixes in the end of this report.

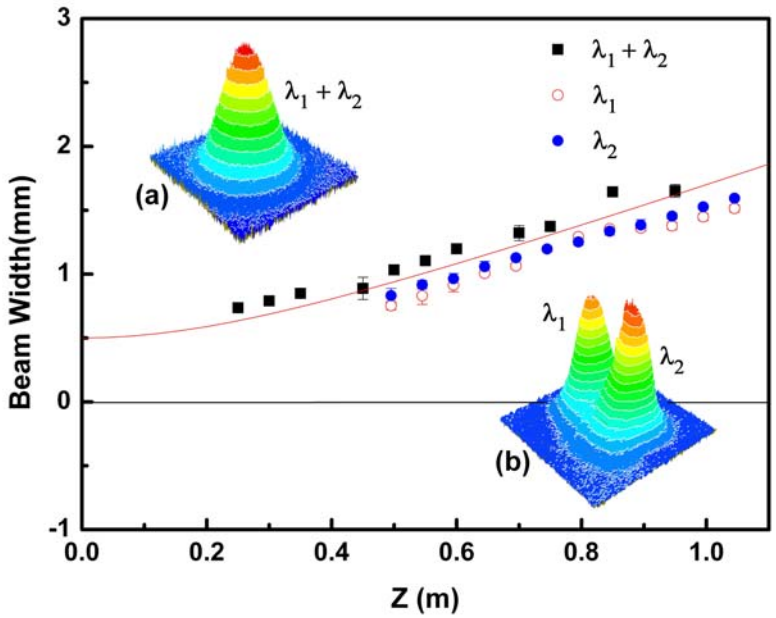

Fig. 5 The beam width as function of the distance (z) from output coupler (M3 in Fig. 4). The solid line represents $w\sqrt{1+(\lambda z/\pi w^2)^2}$ *, where w = 0.3 mm and λ = 800 nm. The insets show the spatial mode of the output laser beam from the collinear tunable dual-wavelength CW Ti:sapphire laser. (a) Measured just after the output coupler (M3 in Fig. 4) without additional prisms. (b) Measured after one prism set just after the output coupler for the separation of the two wavelength components in free space.*

Moreover, the transmissivity of the various S-doped GaSe crystals in far-IR and mid-IR has been measured by Fourier Transform Infrared Spectroscopy (FTIR). Figure 6 shows the transmission spectra of $GaSe_{1-x}S_x$ crystals. The transmissivity between 15 μm and 230 μm decreases as increasing the content of S from x = 0.02 to x = 0.22. However, the transmissivity goes up while further increasing the content of S to x = 0.3 and 0.4. Additionally, the strong absorption has been observed from 22 μm to 70 μm.

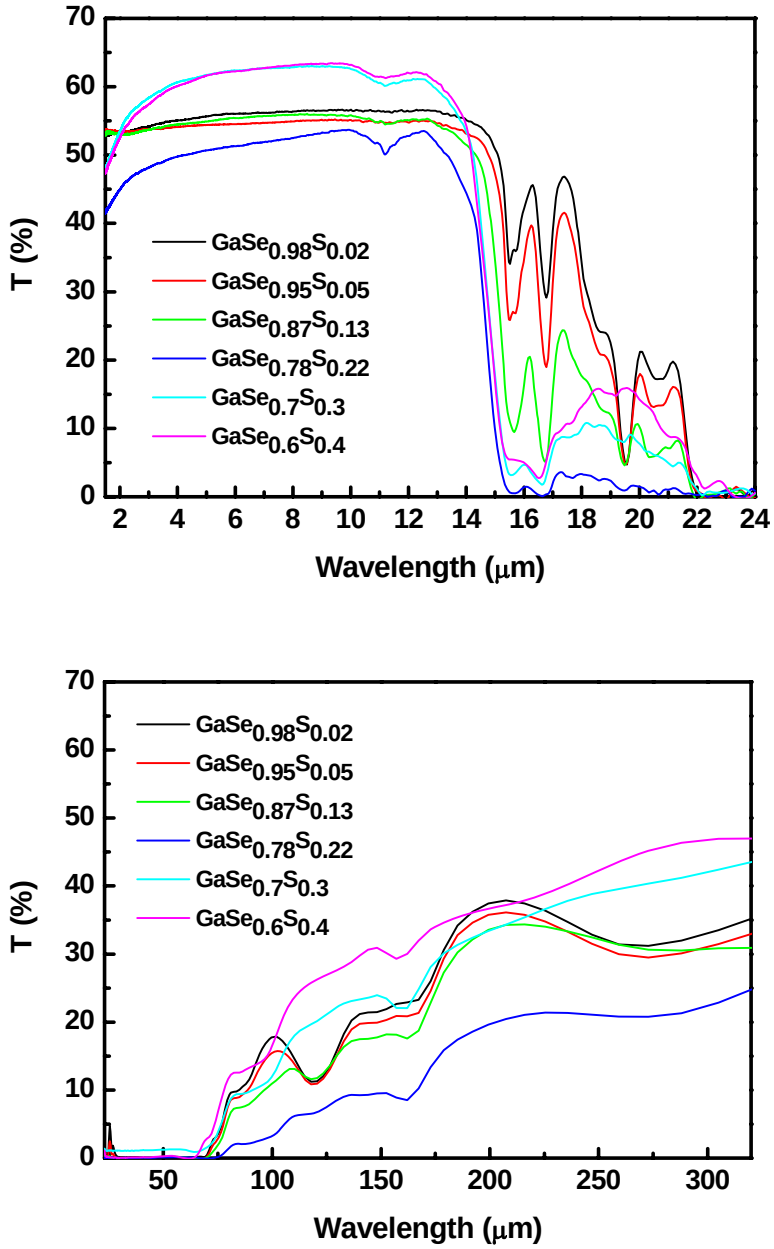

Fig. 6 Transmission spectra of various S-doped GaSe crystals. Curves identification is given in the inset.

2. References:

[1] The cover picture of Rensselear Magazine, http://www.rpi.edu/change/zhang.html.

[2] D. H. Auston, Appl. Phys. Lett. **26**, 101 (1975).

[3] A. G. Davies *et al.*, Phys. Med. Biol. **47**, 3679 (2002).

[4] M. Tani *et al.*, Meas. Sci. Technol. **13**, 1739 (2002).

[5] X.-C. Zhang *et al*., Appl. Phys. Lett. **56**, 1011 (1990).

[6] F. Klappenberger *et al*., Int. J. of Infrar. and Millim. Waves **24**, 1405 (2003).

[7] G. L. Carr *et al*., Nature **420**, 153 (2002).

[8] Ruedeger Koehler *et al*., Nature **417**, 156 (2002).

[9] W. Shi *et al*., Appl. Phys. Lett. **84**, 1635 (2004).

[10] W. Shi *et al*., Opt. Commun. **233**, 183 (2004).

Publication list：

1. **C. W. Luo**, Y. Q. Yang, I. T. Mak, Y. H. Chang, K. H. Wu and T. Kobayashi, 2008 February, *A widely tunable dual-wavelength CW Ti:sapphire laser with collinear output*, Opt. Express 16, 3305 ~ 3309.
   SCI, NSC 96-2923-M-009-001-MY3

3. Self-evaluation:

In this Taiwan-Russia Research Cooperation project, the researchers in Russia started to grow the various S-doped GaSe crystals last year. All of the specimens have been delivered to Taiwan in this March. After received the specimens from Russia, we immediately measured the transmissivity of all crystals in Far-IR and Mid-IR region by Fourier Transform Infrared Spectroscopy (FTIR). Then we try to generate THz radiation from these GaSe:S crystals. Due to more measurements are proceeding, we believe that more results about THz generation will come out soon. Up to now, all of above results achieve about 80 percent of the first-year schedule in this Taiwan-Russia Research Cooperation project. Moreover, we have developed a collinear output and tunable dual-wavelength CW Ti:sapphire laser for generating THz which has been published in Opt. Express in this February.

Appendix

A widely tunable dual-wavelength CW Ti:sapphire laser with collinear output

C. W. Luo,[1*] Y. Q. Yang,[1] I. T. Mak,[1] Y. H. Chang,[1] K. H. Wu,[1] and T. Kobayashi[1,2]

[1]*Department of Electrophysics, National Chiao-Tung University, Hsinchu, Taiwan, R.O.C.*

[2]*Department of Applied Physics and Chemistry and Institute for Laser Science, The University of Electro-Communications, Tokyo , Japan*

[*]*Corresponding author: cwluo@mail.nctu.edu.tw*

Abstract: We report a collinear output and tunable dual-wavelength CW Ti:sapphire laser with a simple cavity configuration. The wavelength splitting range is easily tuned from 10 nm to 110 nm, which provides 56 THz bandwidth for terahertz generation. The total output power of two colors with the spatial mode of TEM_{00} is between 700 mW and 300 mW, for small and large wavelength splittings, respectively, under 5 W argon-ion laser pumping.

OCIS codes: (140.3580) Lasers, solid-state; (140.3590) Lasers, titanium; (140.3600) Lasers, tunable

References and links

1. D. H. Auston, "Picosecond optoelectronic switching and gating in silicon, " Appl. Phys. Lett. **26,** 101–103 (1975).
2. A. G. Davies, E. H. Linfield, and M. B. Johnston, "The development of terahertz sources and their applications," Phys. Med. Biol. **47,** 3679–3689 (2002).
3. M. Tani, M. Herrmann, and K. Sakai, "Generation and detection of terahertz pulsed radiation with photoconductive antennas and its application to imaging," Meas. Sci. Technol. **13,** 1739–1745 (2002).
4. G. L. Carr, Michael C. Martin, Wayne R. McKinney, K. Jordan, George R. Neil, and G. P. Williams, "High-power terahertz radiation from relativistic electrons," Nature **420,** 153–156 (2002).
5. R. Koehler, A. Tredicucci, F. Beltram, H. E. Beere, E. H. Linfield, A. G. Davies, D. A. Ritchie, R. C. Iotti, and F. Rossi, "Terahertz semiconductor-heterostructure laser," Nature **417,** 156–159 (2002).
6. M. R. X. de Barros and P. C. Becker, "Two-color synchronously mode-locked femtosecond Ti: sapphire laser," Opt. Lett. **18,** 831–833 (1993).
7. J. M. Evans, D. E. Spence, D. Burns, and W. Sibbett, "Dual-wavelength self-mode-locked Ti: sapphire laser," Opt. Lett. **18,** 1074–1076 (1993).
8. D. R. Dykaar, S. B. Darack, and W. H. Knox, "Cross-locking dynamics in a two-color mode-locked Ti: sapphire laser," Opt. Lett. **19,** 1058–1060 (1994).
9. A. Leitenstorfer, C. F?rst, and A. Laubereau, "Widely tunable two-color mode-locked Ti : sapphire laser with pulse litter of less than 2 fs," Opt. Lett. **20,** 916–918 (1995).
10. R. A. Kaindl, D. C. Smith, M. Joschko, M. P. Hasselbeck, M. Woerner, and T. Elsaesser, "Femtosecond infrared pulses tunable from 9 to 18 μm at an 88-MHz repetition rate," Opt. Lett. **23,** 861–863 (1995).
11. M. Hyodo, M. Tani, S. Matsuura, N. Onodera, and K. Sakai, "Generation of millimeter-wave radiation using a dual-longitudinal-mode microchip laser," Electron Lett. **32,** 1589–1591 (1996).
12. M. Tani, S. Matsuura, K. Sakai, and M. Hangyo, "Multiple-frequency generation of sub-terahertz radiation by multimode LD excitation of photoconductive antenna," IEEE Microwave Guid. Wave Lett. **7,** 282–284 (1997).
13. C. L. Pan and C. L. Wang, "A novel tunable dual-wavelength external-cavity laser diode array and its applications," Opt. Quantum Electron. **28,** 1239–1257 (1996).
14. T. Hidaka, S. Matsuura, M. Tani, and K. Sakai, "CW terahertz wave generation by photomixing using a two-longitudinal-mode laser diode," Electron. Lett. **33,** 2039–2040 (1997).

#91302 - $15.00 USD Received 3 Jan 2008; revised 14 Feb 2008; accepted 18 Feb 2008; published 26 Feb 2008

15. S. Matsuura, M. Tani, and K. Sakai, "Generation of coherent terahertz radiation by photomixing in dipole photoconductive antennas," Appl. Phys. Lett. **70,** 559–561 (1997).
16. E. R. Brown, K. A. McIntosh, K. B. Nichols, and C. L. Dennis, "Photomixing up to 3.8 THz in low-temperature-grown GaAs," Appl. Phys. Lett. **66,** 285–287 (1995).
17. K. A. McIntosh, E. R. Brown, K. B. Nichols, O. B. McMahon, W. F. DiNatale, and T. M. Lyszczarz, "Terahertz photomixing with diode lasers in low-temperature-grown GaAs," Appl. Phys. Lett. **67,** 3844–3846 (1995).
18. P. Chen, G. A. Blake, M. C. Gaidis, E. R. Brown, K. A. McIntosh, S. Y. Chou, M. I. Nathan, and F. Williamson, "Spectroscopic applications and frequency locking of THz photomixing with distributed-Bragg-reflector diode lasers in low-temperature-grown GaAs," Appl. Phys. Lett. **71,** 1601–1603 (1997).
19. F. Siebe, K. Siebert, R. Leonhardt, and H. G. Roskos, "A fully tunable dual-color CW Ti: Al_2O_3 laser," IEEE J. Quantum Electron. **35,** 1731–1736 (1999).

1. Introduction

Recently, there is growing interesting in fields using terahertz (THz) waves, or T-rays, for spectroscopy, imaging, communications, signal processing, and quantum information. By present time one could get THz radiation by dipole antennas [1, 2, 3], free-electron lasers [4], and quantum-cascade lasers [5]. All of these methods have their merits and deficiencies. It is possible to obtain broad-band radiation with microwave lamps, but it is not coherent; free-electron lasers allow to get radiation in wide range and with high output power, but they are not compact and expensive thus being not available for most of research laboratories. A way to create relatively compact and inexpensive coherent terahertz radiation source is heterodyne downconversion, or photomixing of two-wavelength laser beams on a dipole antenna. According to the type of lasers, it could be distinguished into two parts. One is the pulse THz radiation, which could be generated by the mode-locked Ti:sapphire laser with dual-wavelength emission [6, 7, 8, 9] or the ultrabroad spectrum of a single pulse [10]. The other is CW THz radiation generated by the dual-beam laser sources, such as individual lasers with dual- [11] or multi-mode emission [12], coupled-cavity diode lasers [13, 14], two independently operated lasers [15] (Ti:sapphire laser [16], single-mode LD's [17]), or pairs of actively frequency-locked lasers [18]. Amount of these lasers, diode lasers will be a better candidate for many applications. However, Ti:sapphire lasers should not be forgotten in the exploration of new application areas of THz radiation owing to their high output power, excellent frequency stability, operational robustness, and large continuously tuning range in wavelengths. Siebe, et al., [19] first demonstrated the dual-color CW Ti:sapphire laser in a single laser, which provides two parallel beams at independently tunable wavelengths. For the generation of CW THz, nevertheless, one would prefer to run a single laser with collinear two-color output to simplify the optical alignment and increase the efficiency for THz generation. In the following, we describe the structure of a collinear dual-wavelength CW Ti:sapphire laser and the analysis of its performance.

2. Experimental setup

Figure 1 shows the collinear, tunable dual-wavelength, CW Ti:sapphire laser cavity. It consists of a standard X-configuration resonator and was pumped by an argon-ion laser (Coherent Innova 90) with an output power of 5 W. The 5mm-long Brewster-cut Ti:sapphire crystal was doped with Ti^{+3} ions at the relative concentration of 0.1%. The curvature radius of the focusing mirrors (M1 and M2 in Fig. 1), at the both ends of the Ti:sapphire crystal, was 10 cm. Their tilted angles were 9° and 8.5° respectively. The pump beam (Ar^+ laser) was focused onto the crystal by a lens (L1 in Fig. 1) of 10 cm focal length. The reflectivity of output-coupler (M3 in Fig. 1) was 95%, which was coated at 800 nm with 120 nm spanning.

The prime concept is to expand all wavelengths emitted from a Ti:sapphire crystal in free space by the optical dispersion components. Thus it is possible to select the lasing wavelength inside the cavity through a simple mechanism. In our dual-wavelength CW Ti:sapphire laser,

#91302 - $15.00 USD Received 3 Jan 2008; revised 14 Feb 2008; accepted 18 Feb 2008; published 26 Feb 2008

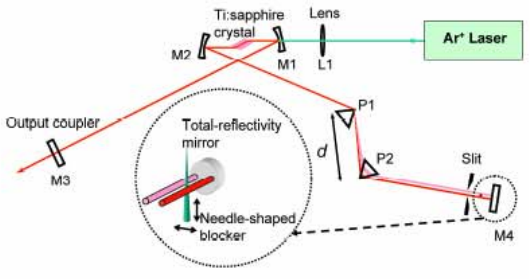

Fig. 1. (Color online) Schematics of the resonator design of the collinear dual-wavelength CW Ti:sapphire laser. M1 and M2 are the curvature mirrors. M3 is the output coupler with 800 nm coating. M4 is the total-reflectivity end mirror. P1 and P2 are the prisms. L1 is the lens for Ar^+ laser. d is the distance between P1 and P2.

a needle-shaped blocker was used as the wavelength selector shown in the inset of Fig. 1. One pair of prisms (P1 and P2 in Fig. 1) was inserted into the long arm of X-configuration resonator to introduce spatial dispersion. The first prism (P1 in Fig. 1) spreads all lasing wavelengths in free space. Then, the second prism (P2 in Fig. 1) guides all of these wavelengths to the total-reflectivity end mirror (M4 in Fig. 1).

To begin with, we adjusted all of the optical components in cavity to optimize the output power in single wavelength operation. Afterward the needle-shaped blocker in front of the total-reflectivity end mirror was moved carefully into the laser beam from the underside of the laser beam. It was separated into two beams between the first prism and the end mirror. The difference of two wavelengths can be tuned by varying the distance between the two beams by adjusting the vertical position of needle-shaped blocker. The collinear and dual-wavelength laser was delivered from the other arm including output-coupler in the X-configuration resonator. Its spectrum has been measured directly by a spectrum analyzer (Advantest, model Q8384).

3. Experimental results

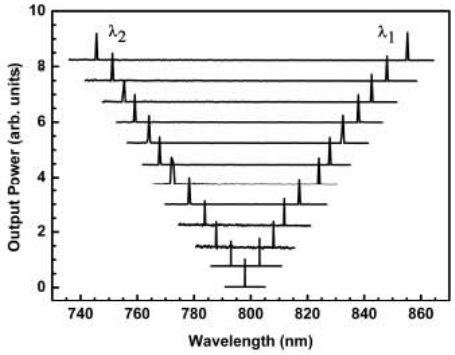

Fig. 2. Spectral separation of the dual-wavelength output of the CW Ti:sapphire laser can be tuned from 10 nm to 110 nm in the case of d = 20 cm (the distance between P1 and P2 in Fig. 1).

#91302 - $15.00 USD Received 3 Jan 2008; revised 14 Feb 2008; accepted 18 Feb 2008; published 26 Feb 2008

Figure 2 shows that the difference between two wavelengths ($\Delta\lambda = \lambda_1 - \lambda_2$) could be continuously tuned from 10 nm to 110 nm by only changing the vertical position of the needle-shaped blocker. Namely, more wavelengths between λ_1 and λ_2 lose as increasing the width of the needle-shaped blocker inside the laser cavity. This wide turning range provides as large bandwidth as 56 THz for the applications of THz generation. Additionally, the two wavelengths could be shifted together with the same separation in wavelength ($\Delta\lambda$) by varying the horizontal position of the needle-shaped blocker. Combining both available operation modes, the different wavelengths with the same separation could properly supply for the THz generation in various types of emitter.

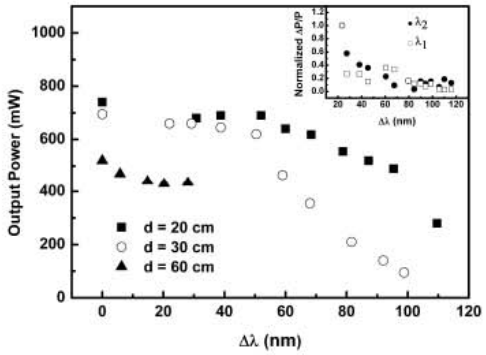

Fig. 3. Total output power of the tunable dual-wavelength CW Ti:sapphire laser as a function of the difference wavelength ($\Delta\lambda$). The solid squares, open circles, and solid triangles represent that the output power in the distance between two prisms (P1 and P2 in Fig. 1) are 20 cm, 30 cm, and 60 cm, respectively. The inset shows $\Delta\lambda$ dependence of the normalized fluctuations of the output power ($\Delta P/P$) for each wavelength.

While the distance (d) between two prisms (P1, P2) is 20 cm, the output power is 740 mW in single wavelength operation as shown in Fig. 3. By increasing the distance between two prisms, however, the output power decreases and the tuning range in $\Delta\lambda$ shrinks. For the case of shorter distance between two prisms, the splitting gap in spectrum between two wavelengths could be as large as 110 nm (solid squares in Fig. 3). On the contrary, the maximum splitting gap in spectrum between two wavelengths is only 30 nm in the case of d = 60 cm (solid triangles in Fig. 3) due to the geometrical restriction of the needle-shaped blocker. The total output power (P, including λ_1 and λ_2) varies slightly below 50 nm in $\Delta\lambda$, but it drops substantially above 50 nm in $\Delta\lambda$. Furthermore, the fluctuations of the output power ($\Delta P/P$, which were estimated from the variation of counts in the spectrometer with 0.2 Hz) in dual-wavelength operation rise clearly especially in smaller $\Delta\lambda$ as shown in the inset of Fig. 3. This indicates that two split wavelengths can independently be amplified by the gain provided in laser cavity in case of larger $\Delta\lambda$ (> 50 nm). On the other hand, two split wavelength modes with smaller $\Delta\lambda$ (< 50 nm) are competing with each other, resulting in the larger fluctuations in the output power. Due to the strong competition of modes around 800 nm, especially, it is hard to achieve dual-wavelength operation under the condition of extremely small splitting (< 10 nm) of two wavelengths. Therefore, the mode competition is concluded to be taking place over ± 25 nm in the laser gain bandwidth of Ti:sapphire. Moreover, the fluctuations of output powers of 845 nm and 760 nm with 85 nm splitting were 11 % and 6 %, respectively, over 2.5 hours.

The inset (a) of Fig. 4 shows that the spatial mode of the tunable dual-wavelength CW

#91302 - $15.00 USD Received 3 Jan 2008; revised 14 Feb 2008; accepted 18 Feb 2008; published 26 Feb 2008

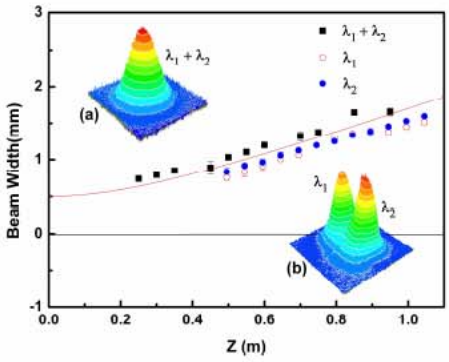

Fig. 4. (Color online) The beam width as function of the distance (z) from output coupler (M3 in Fig. 1). The solid line represents $w(1+(\lambda z/\pi w^2)^2)^{0.5}$, where w = 0.3 mm and λ = 800 nm. The insets show the spatial mode of the output laser beam from the collinear tunable dual-wavelength CW Ti:sapphire laser. (a) Measured just after the output coupler (M3 in Fig. 1) without additional prisms. (b) Measured after one prism set just after the output coupler for separating two wavelength components in free space.

Ti:sapphire laser cavity is TEM_{00} which was measured by the beam profiler just after the output coupler (M3 in Fig. 1). Its propagation along the normal direction of output coupler is Gaussian (solid squares in Fig. 4) and its beam quality (M^2) is 1.28. Furthermore, the same output laser beam had been guided into a prism and measured by the beam profiler after that prism. The spatial modes are still TEM_{00} for both wavelengths, λ_1 = 840 nm and λ_2 = 760 nm, as shown in the inset (b) of Fig. 4. They also propagate along the normal direction of output coupler with Gaussian (solid and open circles in Fig. 4). Additionally, the beam qualities (M^2) of λ_1 (840 nm) and λ_2 (760 nm) are 1.20 and 1.18, respectively. This strongly indicates that the output laser beams of both wavelengths are absolutely collinear. Thus, the collinear output and tunable dual-wavelength CW Ti:sapphire laser could provide many benefits to the dual-wavelength applications, such as wide tuning range, high output power, and easy alignment.

4. Summary

In summary, we have demonstrated the collinear output and wide tunable CW dual-wavelength Ti:sapphire laser. The tuning range of the separation between two wavelengths is continuous from 10 nm to 110 nm. The tunable CW dual-wavelength laser could be stable operated except the very small spitting of two wavelengths. The output power in dual-wavelength operation was greater than 300 mW, even for larger $\Delta\lambda$ (110 nm for the case of d = 20 cm) case. Through this high output power and wide tuning range in CW dual-wavelength Ti:sapphire laser, the high power and tunable coherent CW-terahertz radiation could be generated from the phase matched difference frequency conversion in nonlinear crystals or the photomixing in a biased photoconductive antenna fabricated on a film of low-temperature-grown GaAs.

Acknowledgments

This work was supported by the National Science Council of Taiwan, R.O.C. under grant: NSC95-2120-M-009-011, NSC95-2112-M-009-011-MY3, NSC96-2923-M-009-001-MY3, and by the Grant MOE ATU Program at NCTU.

#91302 - $15.00 USD Received 3 Jan 2008; revised 14 Feb 2008; accepted 18 Feb 2008; published 26 Feb 2008